

## Preparation of a Ferrofluid Using Cyclodextrin and Magnetite

Alberto Bocanegra-Diaz, Nelcy D. S. Mohallem and Rubén D. Sinisterra\*

Departamento de Química, ICEx, Universidade Federal de Minas Gerais, Avenida Antônio Carlos 6627,  
31270-901 Belo Horizonte - MG, Brazil

Um ferrofluido foi obtido a partir da magnetita e da  $\beta$ -ciclodextrina, com a formação de um complexo de inclusão. A caracterização físico-química do complexo magnetita:  $\beta$ -ciclodextrina foi realizada através de espectroscopia de absorção na região do infravermelho com transformada de Fourier, difração de raios X, análise térmica (TG/DTA), microscopia eletrônica de transmissão (TEM) e espectroscopia de absorção atômica. É a primeira vez que se relata na literatura a formação de um complexo de inclusão de um óxido metálico em ciclodextrinas

A ferrofluid has been obtained from magnetite and  $\beta$ -cyclodextrin, with the formation of an inclusion complex. The magnetite and  $\beta$ -cyclodextrin complex was characterized by FTIR spectroscopy, X-ray diffraction, thermal analysis (TG/DTA), transmission electron microscopy (TEM) and atomic absorption spectroscopy. As far as we know, this is the first report on an inclusion compound between a metal oxide and cyclodextrins.

**Keywords:** ferrofluid, cyclodextrin, magnetite, magnetic materials, inclusion complex

### Introduction

Ferrofluids are colloidal suspensions composed of single-domain magnetic nanoparticles dispersed in appropriate solvents (polar or non polar).<sup>1</sup> Since their discovery in 1965 by Papell,<sup>2</sup> ferrofluids have raised a growing interest in the scientific and industrial communities due to their physical properties and applications. Ferrofluids can be applied to immunoassay, cell separation, contrast agents for ultrasound and magnetic resonance imaging (MRI), magnetic inks, biosensors, magnetic microactuators, seals, bearing dampers and lubricants, etc.<sup>3</sup>

These specialized applications of ferrofluids impose strict requirements on their characteristics, such as chemical composition, size distribution uniformity, crystal structure, stability of magnetic properties, surface structure, adsorption properties, solubility and low toxicity.<sup>4</sup>

Many of these properties depend decisively on particle size, shape, composition and structure, and therefore rigorous control of the synthesis of ferrofluids is necessary.<sup>5</sup>

Cyclodextrins are water-soluble oligosaccharides composed of at least six (1-4) linked  $\alpha$ -D-glucosyl residues which have the shape of a hollow, truncated cone, capable of forming inclusion complexes with a variety of guest molecules in the solid state, as well as in solution, with sizes compatible with the dimensions of the cavity.<sup>7</sup> Cyclodextrins are used as surfactants and size controllers of different kind of materials.<sup>6</sup>

In the present work, we describe the preparation and characterization of a ferrofluid using  $\beta$ -cyclodextrin to stabilize magnetite nanoparticles in colloidal suspension. In this system,  $\beta$ -cyclodextrin may also act as a size selector.

### Experimental

Analytical grade chemicals and deionized water were used throughout.

#### *Synthesis of magnetite*

Magnetite was obtained by the coprecipitation method. In brief, 50 mL of an aqueous solution of  $\text{FeSO}_4 \cdot 7\text{H}_2\text{O}$  and  $\text{Fe}_2(\text{SO}_4)_3 \cdot 5\text{H}_2\text{O}$  in 1:1 molar ratio was mixed under vigorous and continuous stirring with 100 mL

\* e-mail: ruben@dedalus.lcc.ufmg.br

of  $\text{NH}_4\text{OH}$ ,  $8.5 \text{ mol L}^{-1}$  as precipitant agent. The resulting black powder was washed several times with water until neutralization, and dried in air at  $110 \text{ }^\circ\text{C}$ . Elemental analysis: Calcd for  $\text{Fe}_3\text{O}_4 \cdot \text{H}_2\text{O} \cdot \text{Fe}$ , 67.1; H, 0.80; O, 32.0%; Found: Fe, 66.8; H, 0.84; O, 32.30%.

#### Preparation of the magnetic fluid

The preparation of the magnetic fluid was carried out by mixing 2.8 mg of  $\beta$ -cyclodextrin and 8.0 mL of  $\text{NH}_4\text{OH}$  ( $8.5 \text{ mol L}^{-1}$ ) dissolved in 15.0 mL of deionized water under continuous and vigorous stirring. The resulting solution was heated to  $40 \text{ }^\circ\text{C}$ , and 2.0 mg of magnetite was slowly added. The system was kept at  $40\text{--}50 \text{ }^\circ\text{C}$ , resulting in a black suspension with pH 7, which was dried at  $60 \text{ }^\circ\text{C}$  in air to form a black powder nanocomposite. Elemental analysis: Calcd for  $\text{Fe}_3\text{O}_4 (\text{C}_{42}\text{O}_{35}\text{H}_{70}) \cdot \text{H}_2\text{O}$ : Fe, 12.1; C, 36.4; O, 46.2; H, 5.2%; Found: Fe, 11.40; C, 34.75; O, 47.87; H, 5.98%.

#### Physical mixture of magnetite and $\beta$ -cyclodextrin

For comparison with the solid nanocomposite, a physical mixture (PM) of  $\beta$ -cyclodextrin and magnetite in the same molar ratio was prepared without heating.

## Methods

In order to verify the stability of the ferrofluid, some physical and chemical tests were carried out, namely, centrifugation, sedimentation and stirring in the presence of a magnet.

The metal contents of the complex were determined on a Hitachi Z 8200 atomic absorption spectrophotometer. The pH measurements were carried out with universal indicative paper (Merck). Elemental analysis was performed using a Perkin-Elmer apparatus model PE2400.

X-ray powder diffraction (XRD) patterns were recorded at  $25 \text{ }^\circ\text{C}$  with a Rigaku-Geigerflex diffractometer using  $\text{Cu-K}\alpha$  radiation ( $\lambda=0.154056 (1) \text{ \AA}$ ). Graphite monochromator was used, in order to increase the analysis efficiency. Data were collected in the  $2\theta$  mode, with  $2\theta$  ranging from  $4$  to  $60^\circ$  in  $0.05^\circ$  steps. Due to crystallinity differences of the samples (ferrite, ferrofluid and  $\beta$ -cyclodextrin), an optimization of the data collection was necessary in order for reasonable quality XRD patterns to be obtained. Nanoparticle size was estimated using the Debye-Scherrer equation ( $D_{\text{hkl}}=0.9\lambda/\beta\cos\theta$ ), in which  $\beta$  stands for the half width of the XRD diffraction line.<sup>8</sup>

Infrared spectra were recorded in the  $4000\text{--}400 \text{ cm}^{-1}$

range with a Galaxy 300 Mattson FT-IR infrared spectrometer, using KBr disks.

Simultaneous thermogravimetric and differential temperature analyses (TG/DTA) were obtained with TA instrument SDT 2060 system in alumina microcrucibles under dynamic  $\text{O}_2$  atmosphere and a heating rate of  $10 \text{ }^\circ\text{C min}^{-1}$ .

Transmission electron micrographs (TEM) were obtained on a Carl Zeiss CEM 902 microscope. Samples were prepared by placing drops of ferrofluid on a copper grid coated with carbon film and dried in air. The nanocomposites (dried ferrofluid) were also analyzed. Spontaneous magnetization was determined on a portable magnetometer.<sup>9</sup>

## Results and Discussion

The obtained ferrofluid was dark brown, exhibited positive magnetic behavior in the presence of a permanent magnet, and kept its colloidal characteristics for up to 12 months. Ferrofluid sedimentation was not observed when the sample was submitted to  $14,000 \text{ rpm}$  centrifugation for 5 min at  $27 \text{ }^\circ\text{C}$ . This result suggests that the magnetite and  $\beta$ -cyclodextrin colloidal solution was stable. The ferrofluid with particle size  $< 2 \text{ nm}$  formed branched or dendritic structures (Figure 1).

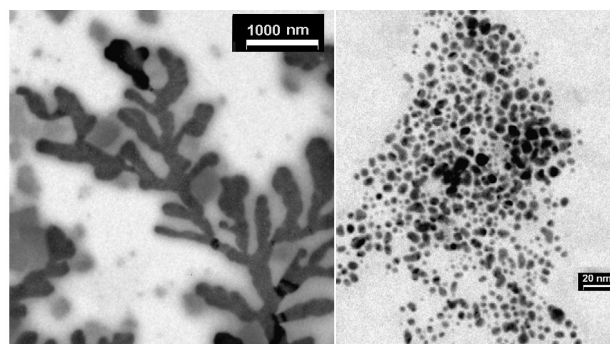


**Figure 1.** TEM micrographs of the ferrofluid emulsion.

The FTIR spectrum of the nanocomposite (Figure 2d) shows bands at  $575$  and  $450 \text{ cm}^{-1}$ , associated with the stretching and torsional vibration modes of the magnetite Fe-O bonds in tetrahedral and octahedral sites, respectively (Table 1). The attributions are in accordance with Keiser *et al.*<sup>10</sup> and Poling,<sup>11</sup> who described two broad bands at  $580$  and  $400 \text{ cm}^{-1}$  associated with magnetite. The absorptions in the  $846\text{--}1640 \text{ cm}^{-1}$  range are related to the characteristic vibrations of  $\beta$ -cyclodextrin (Figure 2a), suggesting that the  $\beta$ -cyclodextrin structure remains intact upon reaction.

Another important observation was the sharp decrease of the intensity of the  $\nu_{\text{O-H}}$  band at  $3400 \text{ cm}^{-1}$  in the

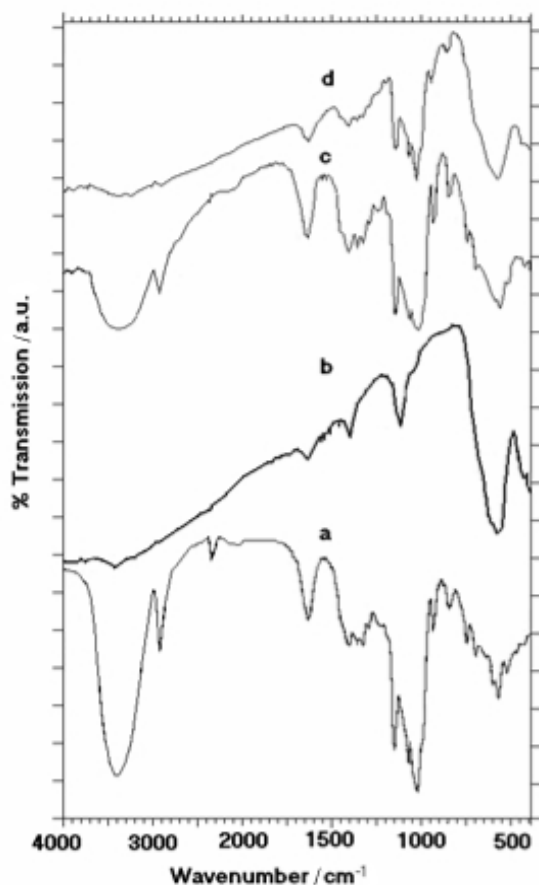


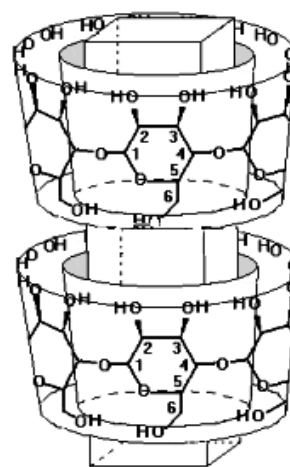
**Figure 2.** IR spectra of: a-  $\beta$ -cyclodextrin, b- magnetite, c- the physical mixture (PM) of  $\beta$ -cyclodextrin and magnetite, d- nanocomposite.

**Table 1.** Infrared absorption frequencies ( $\text{cm}^{-1}$ ) of  $\beta$ -cyclodextrin and of ferrofluid

$\beta$ -cyclodextrin	Ferrofluid	Tentative Assignment
3512		$\nu(\text{OH})$ of primary OH groups $\gamma$
3342		$\nu(\text{OH})$ of secondary OH groups
3196		H-bonded in different ways
3107		
1650	1650	$\delta(\text{HOH})$ of two different types of water molecules existing in the cavities
1459	1459	$\phi(\text{OCH})$ , $\phi(\text{HCH})$
1420	1420	$\phi(\text{OCH})$ , $\phi(\text{CCH})$
1398		$\phi(\text{CCH})$ , $\phi(\text{OCH})$ , $\phi(\text{COH})$
1158	1158	$\nu(\text{C-O-C})$
1100	1100	$\nu(\text{C-O-C})$
	575	$\nu(\text{Fe-O})$
	450	$\nu(\text{Fe-O})$

spectrum of the nanocomposite. In contrast, this vibration can be clearly observed in the spectra of the  $\beta$ -cyclodextrin and of the physical mixture (PM) (Figure 2a, 2c). This decrease could be interpreted as resulting from total

deprotonation of the hydroxyl groups of  $\beta$ -cyclodextrin in the nanocomposite, as described in the literature.<sup>12</sup> However, Wenz<sup>13</sup> reported the need of drastic chemical conditions such as high temperature, strong reducing agent (NaH) and absence of water for the deprotonation of  $\beta$ -cyclodextrin to occur, which is not the case in our work. On the other hand, in accordance with previous works the suppression of -OH vibrational modes in the 3000-3700  $\text{cm}^{-1}$  region has been related to evidence of host-guest interaction as a consequence of complete water release upon inclusion.<sup>14,15</sup> Hence we can suggest the inclusion of magnetite into the  $\beta$ -cyclodextrin cavity, (Scheme 1). This hypothesis was also confirmed by our previous magnetic results published elsewhere.<sup>16</sup>



**Scheme 1.** Proposed magnetite inclusion into  $\beta$ -cyclodextrin cavity.

The infrared spectrum of the physical mixture clearly shows predominance of  $\beta$ -cyclodextrin vibrations and overlapping of the magnetite bands (Figure 2b).

The diffractogram of the nanocomposite (Figure 3d) suggests the presence of a new crystalline phase in contrast to the XRD pattern of PM (Figure 3c), magnetite (Figure 3b) and  $\beta$ -cyclodextrin (Figure 3a). The presence of  $\beta$ -cyclodextrin and magnetite characteristic reflections indicated the maintenance of the cyclodextrin and magnetite crystallographic organization in the nanocomposite. These results could suggest a column crystalline organization of the inclusion compound (Scheme 2a and 2b) as observed by MacMullan *et al.*<sup>17</sup>

Thermal analysis data reinforce the hypothesis of inclusion of magnetite into  $\beta$ -cyclodextrin. The TG curve of  $\beta$ -cyclodextrin (Figure 4a) shows a thermal decomposition behavior, as discussed elsewhere.<sup>14</sup> The DTA curve of  $\beta$ -cyclodextrin (Figure 5a and insert) shows two endothermic events at 85 and 303  $^{\circ}\text{C}$ , and two

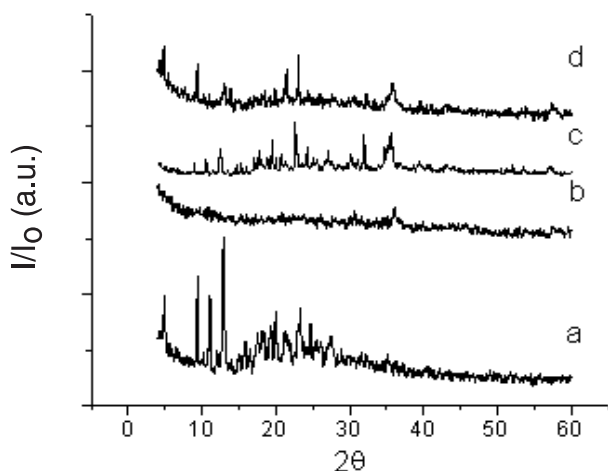
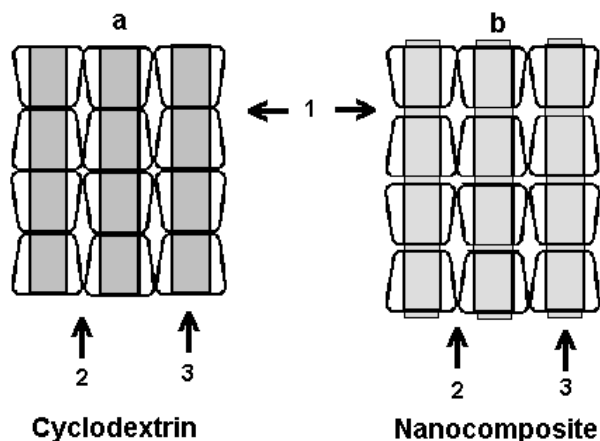


**Figure 3.** XRD pattern of: a-  $\beta$ -cyclodextrin, b- magnetite, c- the physical mixture (PM) of  $\beta$ -cyclodextrin and magnetite, d- nanocomposite.



**Scheme 2.** Graphic representation of the channel-like arrangement of  $\beta$ -cyclodextrin (a) and of the nanocomposite supported by the dipole-dipole interactions of the included magnetite (b).

exothermic events at 345 and 480 °C, respectively. The event at 85 °C is associated with the loss of water molecules (17%), as verified in the respective TG curve. The endothermic event at 303 °C could be associated with the oligosaccharide fusion followed by thermal decomposition between 345–485 °C (83% of weight loss).

The TG curve of the nanocomposite (Figure 4c) resembles the  $\beta$ -cyclodextrin thermal decomposition profile, but a final residue of 46% was observed. In comparison, the PM (Figure 4b) and  $\beta$ -cyclodextrin (Figure 4a) TG curves present 12% and no residue, respectively. The nanocomposite DTA curve (Figure 5c) reveals two thermal events, a small wide endothermic peak at 97 °C, and an exothermic peak at 350 °C. The first peak could be associated with the loss of water (9%), which was also verified in the respective TG curve. The exothermic peak

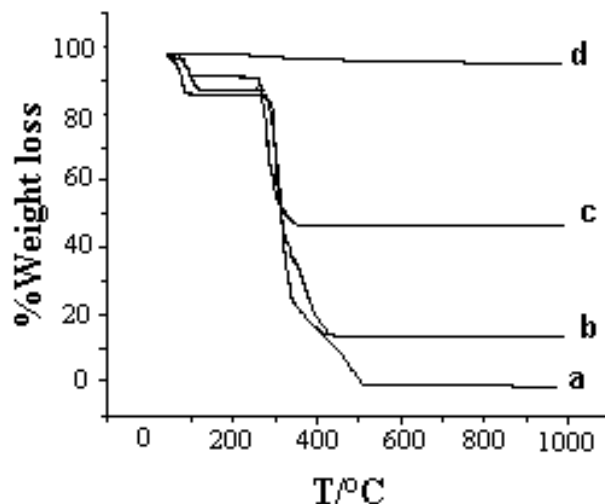


**Figure 4.** TG curves of (a)  $\beta$ -cyclodextrin, (b) the physical mixture (PM) of  $\beta$ -cyclodextrin and magnetite in 1:1 molar ratio, (c) nanocomposite, and (d) magnetite.

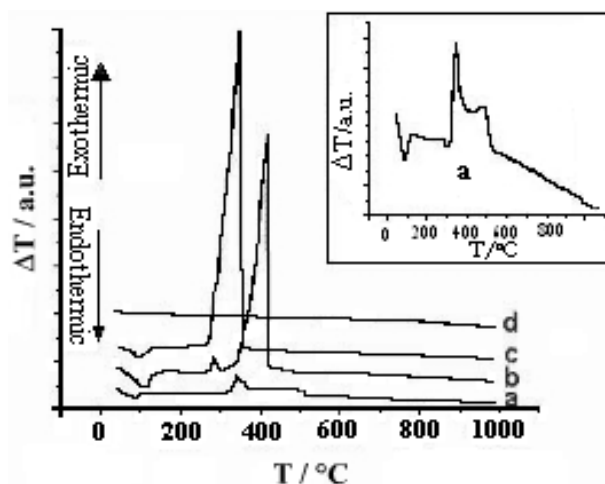


**Figure 5.** DTA curves of (a)  $\beta$ -cyclodextrin, (b) the physical mixture (PM) of  $\beta$ -cyclodextrin and magnetite in 1:1 molar ratio, (c) nanocomposite, and (d) magnetite. Insert DTA of  $\beta$ -cyclodextrin.

is in accordance with the total thermal decomposition of the nanocomposite.

In contrast, the PM TG curve (Figure 4b) resembles quite well the  $\beta$ -cyclodextrin thermal decomposition profile. The PM DTA curve (Figure 5b) showed a single endothermic peak at 110 °C and two exothermic events at 285 and 415 °C, respectively. The first peak is attributed to water loss (12%), and the next two peaks could be associated respectively to the occurrence of some interaction between  $\beta$ -cyclodextrin and magnetite in the PM and the  $\beta$ -cyclodextrin thermal decomposition process (76% of weight loss).

The fluid density and spontaneous magnetization of the nanocomposite were 8.48 g L<sup>-1</sup> and 4.4 A m<sup>2</sup> kg<sup>-1</sup>,

respectively. The lower value of the spontaneous magnetization in comparison with that of magnetite ( $90 \text{ A m}^2 \text{ kg}^{-1}$ ) suggests that both the magnetic fluid and the nanocomposite could be used in bioprocessing isolation of monoclonal antibodies from ascite fluid or from culture<sup>3</sup> and as a contrast agent in MRI and ultrasound,<sup>18</sup> among other applications.

Finally, the transmission electronic microscopy (TEM) of the nanocomposite shows a series of aligned magnetite particles (Figure 6). The literature reports the use of surfactants as cyclodextrins and micelles as templates for the control of nanoparticle size and shape.<sup>6,18-20</sup> Hence, we suggest, therefore, that cyclodextrin plays a similar role in the control of the magnetite particle shape and size, in the present case through the inclusion of magnetite into the  $\beta$ -cyclodextrin cavity.

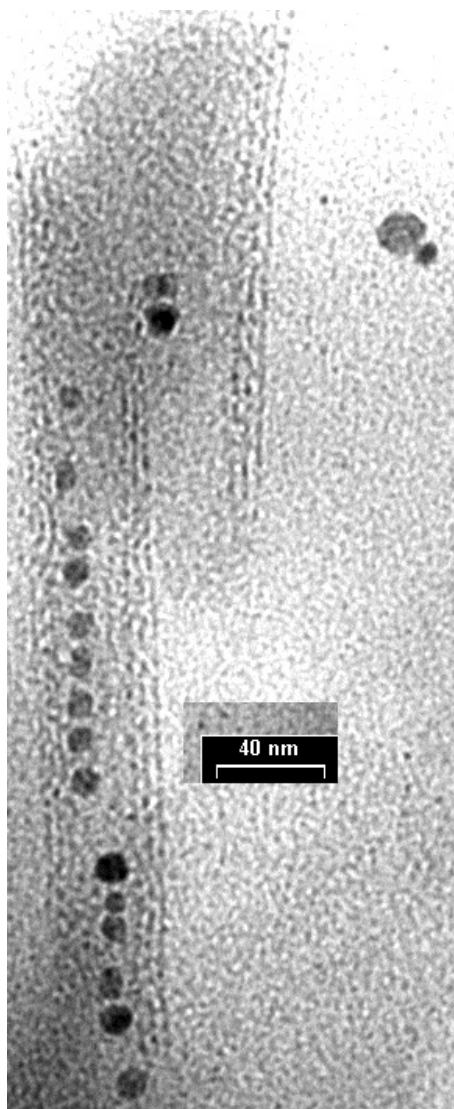


**Figure 6.** TEM micrographs of solid state nanocomposite. The dark objects are magnetite.

## Conclusion

A new ferrofluid compound was obtained and characterized from magnetite and  $\beta$ -cyclodextrin. To the best of our knowledge, this is the first report in the literature on the inclusion of metallic oxides into  $\beta$ -cyclodextrin. The present work strongly suggests the key role of cyclodextrins in the control of the magnetite shape and nanosize through its inclusion into the  $\beta$ -cyclodextrin cavity.

## Acknowledgements

The authors would like to thank the Dr. N. Spezialli of Departamento de Física - UFMG for XRD analyses, Dr. F. Galembeck of Instituto de Química - UNICAMP for TEM micrographs, and the financial support of the Brazilian agencies CAPES and CNPq.

## References

- Shen, F.; Laibinis, P. E.; Hatton, T.A.; *J. Magn. Magn. Mat.* **1999**, *194*, 37.
- Papell, S.S.; *U.S. Pat* 3,215,572, **1965**.
- Bocanegra-Diaz, A.; Mohallem, N.D.S.; Sinisterra, R.D; *PCT/BR* 02/00155, **2002**; Molday R. S.; *U.S. Pat* 4,452,773, **1982**; Pilgrim, H.; *U.S. Pat* 6,274,121, **2001**; Groman, E.V.; Josephson, L.; Lewis, J.M; *U.S. Pat* 4,951,675, **1990**; Cockbain, J.; *WO* 97/25073, **1997**; Liberti, P.A.; Rao, G.C.; Chiarappa, J.N.; *U.S. Pat* 6,120,856, **2000**; Kovac, Z.; Gardineer, B.A.; *U.S. Pat* 3,990,981, **1976**; Sambucetti, C.J; Mitchell, J.W.; *U.S. Pat* 4,026,713, **1977**; Kovac, Z.; Sambucetti, C.J.; *U.S. Pat* 4,107,063, **1978**; Pérez-Castillejos, R.; Plaza, J.A.; Losantos, E.P.; Acero, M.C.; Cané, C.; Serra-Mestres, F.; *Sens. Actuators, A* **2000**, *84*, 176.
- Kuznetsov, O. A.; Brusentsov, N. A.; Kuznetsov, A. A.; Yurchenko, N.Y.; Osipov, N. E.; Bayburtskiy, F.S.; *J. Magn. Magn. Mat.* **1999**, *194*, 83.
- Gruttner, C.; Rudershausen, S.; Teller, J.; *J. Magn. Magn. Mat.* **2001**, *225*, 1; Yu, L.Q.; Zheng, L.J.; Yang, J.X.; *Mat. Chem. Phys.* **2000**, *66*, 6; Kim, D.K.; Zhang, Y.; Voit, W.; Rao, K.V.; Muhammed, M.; *J. Magn. Magn. Mat.* **2001**, *225*, 30; Gruttner, C.; Teller, J.; *J. Magn. Magn. Mat.* **1999**, *194*, 8; Zins, D.; Cabuil, V.; Massart, R.; *J. Mol. Liq.* **1999**, *83*, 217; Facounnier, N.; Bée, A.; Roger, J.; Pons, J.N.; *J. Mol. Liq.* **1999**, *83*, 233; Massart, R.; Cabuil, V.; *J. Chim. Phys.* **1987**, *84*, 967; Pileni, M.P.; *Nature* **2003**, *2*, 145.
- Bardi, L; Mattei, A.; Steffan, S.; Marzona, M.; *Enz. Mic. Tech.* **2000**, *27*, 709.
- Saenger, W.; *Angew. Chem. Int. Ed. Engl.* **1980**, *19*, 344; Cortés, M. E.; Sinisterra, R.D.; Avila-Campo, M.J.; Tortamano,

- N.; Rocha, R.G.; *J. Inclusion Phenom. Macrocyclic Chem.* **2001**, *40*, 297; Beraldo, H.; Sinisterra, R.D.; Teixeira, L.R.; Vieira, R.P.; Doretto, M.C.; *Biochem. Biophys. Res. Commun.* **2002**, *296*, 241; Sinisterra, R.D.; Najjar, R.; Santos, P.S.; Alves, O.L.; Alves de Carvalho, C.A.; Munson, E.; Thakur, C.; *Mol. Recog. Incl.* **1998**, 511.
8. Cullity, B. D.; *Elements of X-ray Diffraction*, A. W. P. C, Inc: Massachusetts, 1967.
9. Coly J. M. D.; Fabris J. D; *Rev. Fis. Apl. Instr.* **1982**, *7*, 25.
10. Keiser, J.T.; Brown, C.W.; Heidersbach, R.H.; *J. Electrochem. Soc.* **1982**, *129*, 2686.
11. Poling, G.W.; *J. Electrochem. Soc.* **1969**, *116*, 958.
12. Fuchs, R.; Habermann, N; Klufers, P.; *Angew. Chem. Int. Ed. Engl.* **1993**, *32*, 852.
13. Wenz, G.; *Angew. Chem. Int. Ed. Engl.* **1994**, *33*, 803.
14. Sinisterra, R.D.; Najjar, R.; Alves, O.L.; Santos, P.S.; Alves de Carvalho, C.A.; Conde da Silva, A.L.; *J. Inclusion Phenom. Mol. Rec. Chem.* **1995**, *22*, 91.
15. Bocanegra, A.; Mohallem, N.D.S.; Sinisterra, R.D.; *Mat. Res. Soc. Symp. Proc. 711*, **2002**, 30.1.
16. Bocanegra, A.; Novak, M., Mohallem, N.D.S.; Sinisterra, R.D.; *J. Magn. Magn. Mater.* **2003**, in press.
17. McMullan, R.K.; Saenger, W.; Fayes, J.; Mootz, O.; *Carbohydr. Res.* **1973**, *31*, 37.
18. Kohata, S.; Jyodoi, K.; Ohyoshi, A.; *Thermochim. Acta* **1993**, *217*, 187.
19. Klaveness, J.; Rongved, P.A.; Stubberud, L.; *U.S. Patent* 5,928,626, **1999**.
20. Whaley, S. R.; English, D.S.; Hu, E.L.; Barbara, P.F.; Belecher, A. M.; *Nature* **2000**, *405*, 665; Kumar, R.V.; Kolytyn, Y.; Xu, X.N.; Yeshurun, Y.; Gedanken, A. and Felner, I.; *J. Appl. Phys.* **2001**, *89*, 6324; Sun, S.; Murray, C.B.; Dieter, W.; Folks, L.; Moser, A.; *Science* **2000**, *287*, 1989; Puntès, V.F.; Krishnan, K.M.; Alivisatos, A. P.; *Science* **2001**, *291*, 2115; Philp, D.; Stoddart, F.; *Angew. Chem. Int. Ed. Engl.* **1996**, *35*, 1155.

Received: May 16, 2003

Published on the web: December 10, 2003